NASA Contractor Report 3984

NASA-CR-3984 19860015190

Vapor-Screen Flow-Visualization Experiments in the NASA Langley 0.3-m Transonic Cryogenic Tunnel

Gregory Vincent Selby

GRANT NGT 47-003-029
MAY 1986

NASA Contractor Report 3984

Vapor-Screen Flow-Visualization Experiments in the NASA Langley 0.3-m Transonic Cryogenic Tunnel

Gregory Vincent Selby
Old Dominion University
Norfolk, Virginia

Prepared for
Langley Research Center
under Grant NGT 47-003-029

National Aeronautics
and Space Administration

**Scientific and Technical
Information Branch**

1986

FOREWORD

This report covers the work completed on the research project, "Vapor-Screen Flow-Visualization Experiments in the NASA Langley 0.3-meter Transonic Cryogenic Tunnel," during Summer 1984 and Summer 1985. The work has performed under the NASA-ASEE Summer Faculty Fellowship Program. Dr. Robert M. Hall and Mr. Jerry B. Adcock served as NASA associates/consultants during the program.

ABSTRACT

The vortical flow on the leeward side of a delta-wing model has been visualized at several different tunnel conditions in the NASA Langley 0.3-meter Transonic Cryogenic Tunnel using a vapor-screen flow-visualization technique. Vapor-screen photographs of the subject flow field are presented herein and are interpreted relative to phenomenological implications. Results indicate that the use of nitrogen fog in conjunction with the vapor-screen technique is feasible.

TABLE OF CONTENTS

LIST OF TABLES

LIST OF FIGURES

1.0. INTRODUCTION

1.1. Background

The National Transonic Facility (NTF) has recently become operational. As in most transonic tunnels, experimenters would like to have the capability of visualizing surface and freestream flow fields. Meaningful testing at NTF requires surface flow - visualization techniques that meet specific requirements; e.g., facilitate the identification of shock locations and flow separation patterns.[1,2]

Specific requirements for freestream flow - visualization techniques applicable to a cryogenic environment include:

a. freestream flow patterns must be easily recorded and readily interpreted;

b. freestream indicators must be non-contaminating and cause no interference with the flow field while facilitating the identification of regions of vortical flow and

c. freestream flow patterns must be distinctly perceivable while the tunnel is on-line and capable of being documented into clear permanent records.

These requirements cannot be met, however, due to the current unavailability of functional flow - visualization techniques applicable to the cryogenic environment associated with NTF.

1.2. Literature Review

Understandably, only a few formal flow-visualization studies have been performed in a cryogenic environment, due primarily to the small number of cryogenic facilities accessible to experimental fluid dynamicists and to the

difficulties of having adequate optical access in those tunnels. Notably, techniques for visualizing both surface and freestream flows are presently under development. Relative to surface flow visualization, Kell[3] has successfully used liquid propane as a surface indicator in the Subsonic Cryogenic Wind Tunnel at the University of Southampton. While employed by the McDonnell Douglas Corporation, Crowder[4] examined various liquid and gaseous surface indicators. Fluorescent minitufts, a technique for visualizing surface flows that has been used extensively in conventional tunnels,[5,6] are presently being studied by the Instrument Research Division of NASA Langley Research Center for potential use in a cryogenic environment.

Visualization of freestream cryogenic flow fields, using optical methods, has also been attempted. Burner, et al.[7] have applied the holographic interferometry technique to the NASA Langley 0.3-m Transonic Cryogenic Tunnel. In addition, Rhodes and Jones[8,9] have investigated the use of schlieren, shadowgraph and Moiré deflectometry techniques in the same facility.

Bisplinghoff, Coffin and Haldeman[10] have used a mixture of liquid nitrogen and steam-bearing air to achieve flow visualization in a conventional subsonic wind tunnel. Haldeman[11] has proposed a modification to this technique to produce nitrogen fog for flow visualization in cryogenic wind tunnels. This concept, which has not been experimentally tested, is based on the use of liquid helium to precipitate nitrogen fog in a temperature-controlled nozzle. The resulting neutrally buoyant mixture, obtained through careful adjustment of mixture temperature and nitrogen-to-liquid helium mass ratio, is then injected into the tunnel test section at a temperature near the freestream value.

To the author's knowledge, a systematic study of the use of fog to visualize the flow field in a cryogenic environment has not previously been performed. It is believed that the need for such research has been adequately demonstrated in conference proceedings, such as Reference 1.

1.3. Research Objectives

The overall objective of the present research is to apply the vapor-screen flow-visualization technique[12] to a cryogenic flow field. In order to accomplish this goal, the vapor-screen technique is being used to attempt visualization of the flow over a three-dimensional model in the 0.3-m Transonic Cryogenic Tunnel. It is also intended that the results of this research provide knowledge relative to optimum flow conditions (in terms of Mach number (M), total temperature (T_t) and total pressure (p_t)) for photographically suitable vapor screens.

2.0. EXPERIMENTAL PROGRAM

2.1. Test Facility

The NASA Langley Research Center 0.3-m Transonic Cryogenic Tunnel (TCT) as shown in Figure 1, is a continuous flow, fan-driven tunnel with a removable, 20-cm by 60-cm, two-dimensional test section. The tunnel uses nitrogen as the working gas and cooling is accomplished by the injection of liquid nitrogen into the flow at an injection station located in the upper-leg diffuser section.

With the two-dimensional test section installed, the 0.3-m TCT is capable of operating at temperatures varying from 80 K to 330 K and stagnation pressures ranging from slightly greater than 1 to 6.0 atmospheres. Mach number can be varied from approximately 0.05 to 0.95. The ability to operate at cryogenic temperatures combined with the 6-atm. pressure capability results in an extremely high Reynolds number capability. In addition, pressure and temperature can be uniquely varied independent of Mach number. Additional relevant details of the tunnel and its operation can be found in Reference 13.

2.2. Test Configuration and Tunnel Conditions

The 65-degree half-span delta-wing model shown in Figures 2 and 3 has been tested at the various tunnel conditions listed in Table 1. The subject model had previously been used to perform the tests reported in Reference 14. In the present tests, the model was mounted on a turntable in the test section to accomplish variations in the angle attack (α) from 13 to 30 degrees. In addition, Mach number (M) was varied from 0.4 to 0.8; total pressure (p_t) was varied from 1.3 to 5.0 atmospheres and total temperature (T_t) was varied from 83 to 101 K.

The delta-wing model was previously load tested in conjunction with the buffet tests reported in Reference 14. The maximum normal load applied to the model during the load tests was 490 N which was calculated to be approximately 19% of the load required for failure. If a safety factor (SF) is defined as the ratio of the failure load to a given load, then the safety factor for the load tests (SF_{LT}) was always greater than 5.3. From the equation for the normal aerodynamic force on the wing, an equation can be developed for the maximum allowable dynamic pressure (q_m) at any given angle of attack for a desired value of the safety factor. The resulting equation is:

$$q_m = \frac{N}{C_{L_\alpha}\,\alpha\left(\cos\alpha + \frac{C_D}{C_L}\sin\alpha\right)S}\,\frac{SF_{LT}}{SF}$$

where

N = maximum applied load during load tests

SF_{LT} = SF corresponding to N,

SF = desired value of the safety factor,

C_{L_α} = lift curve slope from Reference 15,

C_L/C_D = lift-to-drag ratio from Reference 15 and

S = wing planform area.

In order to calculate the maximum allowable total pressure (p_{tm}) as a function of angle of attack, values of the ratio q/p_t were obtained from isentropic flow theory. The above equation is presented in graphical form in Figure 4. For example, it can be observed that for SF = 3.0 at M = 0.6 and p_t = 5 atm., the maximum allowable angle of attack is 21.5°. For this value of SF (the one chosen for the present tests), Figure 4 was used to determine the maximum allowable angle of attack at a given value of the total pressure.

While structural considerations led to the angle-of-attack limitations

derived from Figure 4, phenomenological considerations led to additional limitations. In order to maintain a vortex burst location downstream of the trailing edge of the model, Figure 5 (experimental data from Reference 15) indicates that a 20-degree limitation in the angle of attack should be observed. In the present tests, angle of attack was varied between 15 and 30 degrees in an attempt to visualize the vortex-bursting phenomenon.

2.3. Description of Flow-Visualization Technique

The conventional vapor screen flow-visualization technique, described in detail in Reference 12, is being used for the first time to accomplish flow visualization in a cryogenic environment. In the experiments performed to date, this technique has been used to visualize the flow over a 65° half-span delta-wing model at several angles of attack. The delta-wing model was mounted on a turntable in the test section, as shown in Figure 3, in order to provide the capability of varying the angle of attack. Nitrogen fog was generated in the test section by slowly decreasing the stagnation temperature until the freestream temperature approached its saturation value. The presence or absence of fog in the test section was verified visually by observing the flow on a video monitor. The density of the fog was varied (by varying freestream temperature as previously mentioned) in an effort to produce an optimum fog density. Optimal fog density for a given set of model and tunnel conditions (α, M, p_t) was determined qualitatively by viewing the flow on the video monitor. The fog was illuminated by a system designed by personnel in the NASA Langley Instrument Research Division and schematically depicted in Figure 6.

The illumination system is composed of the 15-mW helium-neon laser, focusing mirrors and cylindrical lens, as shown in Figure 7. When the beam of

light from the laser passes through the cylindrical lens, a nearly vertical plane sheet of light is generated and oriented so that it intersects the model between half and full chord. The light sheet is also swept with respect to the tunnel walls in order to facilitate visualization of the three-dimensional vortical-flow structure on the leeward side of the model. Video and still cameras, used to record the visualized flow, were mounted inside an instrumentation pod which was attached to one side of the test section. (See Figures 7 and 8.) Ideally, the light sheet would reside in a vertical plane oriented at an angle of 90° with respect to the line-of-sight of the cameras and the longitudinal axis of the vortex, i.e., the line-of-sight of the camera should be coincident with the longitudinal axis of the vortex. This overall orientation was not possible in the present experiments due to existing physical and geometric constraints. For example, the existing port in the test section ceiling, which held the cylindrical lens box, was located downstream of the trailing edge of the model. Therefore, the plane light sheet had to be inclined with respect to the vertical in order for its plane to intersect the model. In spite of the obstacles that were confronted, it is believed that the photographs presented in the next section will demonstrate the feasibility of the subject flow-visualization technique.

3.0. PRESENTATION AND DISCUSSION OF FLOW VISUALIZATION PHOTOGRAPHS

Several seconds of video data were recorded and two or more still photographs were taken for each case listed in Table 1 after Point 40. During Runs 1, 2 and 3, photographically suitable flow conditions were not attained. This may have been partially due to the fact that condensation began to accumulate on the plenum chamber window at some point during Runs 2 and 3. In addition, toward the completion of Run 3, it was discovered that the Hasselblad camera had jammed because of exposure to cold temperatures. As a result of these complications, no usable data were obtained from the first three runs. Between Runs 3 and 4, the light sheet was moved to an orientation more parallel with the tunnel walls and warm air was ducted to the instrumentation pod in order to prevent the Hasselblad camera from jamming and frost from forming on the plenum chamber window. Adequate video data were obtained after these changes were implemented. However, all the still photographs appear overexposed, though exposure times of 1 and 5 seconds were used. Runs 4 through 7 were performed on two consecutive days and prints of the first day's negatives were not available by the time testing began on the second day. Preliminary inspection of the negatives had led to the conclusion that the exposure times were adequate.

Flow visualization was not possible at M = 0.4 because optimum thermal conditions were not reached before the operating thermal safety limit of the tunnel was approached. At M = 0.8, significant interference was observed in the video signal, possibly due to tunnel vibration. Towards the end of Run 5 (M = 0.8), the video image became increasingly hazy. After Point 49, the Mach number was decreased to 0.6 and the image observed remained hazy though the plenum chamber window was clear upon inspection after tunnel shutdown. One

possible explanation for the haziness is that fog developed in the plenum chamber during Run 5. This phenomenon can occur if the plenum chamber temperature lags the test section temperature by a significant amount.

The flow visualization photographs being presented are for ten points from Runs 4 and 6. These ten cases are summarized in Table 2. The subject flow visualization photographs were reproduced from video tape using a still camera with long exposure time.

The series of photographs presented in Figure 9 illustrate the change in the size of the vortex region as a function of angle of attack at M = 0.6 and p_t = 1.3 atm. A series recorded at the same Mach number, but at p_t = 3.0 atm., is presented in Figure 10. A comparison of these two figures indicates an increase in the size of the vortex region as a function of angle of attack at a constant value of p_t. An increase in vortex region size with increasing p_t at a constant angle of attack is also generally indicated, although whether this is a Reynolds number effect or a condensation rate effect is not known.

Photographs recorded at various Mach numbers at a constant angle of attack of 20° and p_t = 3.0 atm. are presented in Figure 11. This series indicates that the vortex region generally increases with increasing Mach number.

Wakes and vortices from wings usually appear as dark "holes" in a vapor screen, not as a white area against a dark background, as in the present tests. An explanation is offered for this phenomenon. In a conventional vapor screen, total condensation of the finite quantity of water vapor occurs in a region upstream of the model. When the condensation particles reach the test section, radial acceleration produced by circulatory flow exerts a strong centrifuging action on these particles. As a consequence, these fog particles

are usually quickly swept from the center of the vortex creating a dark region against a white background. In the present tests, local or regional condensation occurs due to higher local Mach numbers in the vortex region. It is possible that condensation occurs at a greater rate than the fog particles can be swept away from the vortex core. Consequently, the medium surrounding the vortex area appears black, while the vortex area appears white. This phenomenon has previously been experienced, as reported in Reference 12.

The vortex regions in the present photographs show a lack of definition as compared to the level of detail present in the vortex region in conventional vapor screen photographs. One possibility is that vortex breakdown has occurred upstream of the light sheet at the minimum test angle of attack of 15 degrees. The data presented in Figure 5 from Reference 15 apply directly to a full-span delta-wing model with beveled leading-edge on both sides of the airfoil. The present test configuration (Figure 2) has a beveled leading edge only on the leeward side. Reference 15 also contains data for a full-span delta-wing model with a square leading edge. At a given location between the mid-chord and full chord positions, vortex breakdown occurs at a two to four-degree lower angle of attack for the square leading edge than for the leading edge beveled on both sides. For a 65° full-span delta wing, Figure 5 indicates that vortex bursting occurs at the trailing edge for an angle of 19.5 degrees. The differences in leading-edge geometry and in sidewall boundary-layer influences might reduce this value below the minimum angle of attack of 15° for the present tests. If vortex bursting occurred upstream of the light sheet, a diffuse vortex core would be expected at downstream locations. The corresponding vapor-screen photographs would then be similar to those taken in the present tests.

Conditions for photographically suitable vapor screens have been defined

at M = 0.6 and p_t = 1.3 atm. for the present model. These data are presented Figure 12 for this single case. Data were not obtained for other combinations of tunnel conditions due to a lack of time.

4.0. SUMMARY, CONCLUSIONS AND RECOMMENDATIONS

The vapor-screen flow-visualization technique has been applied to the flow over a 65-degree half-span delta-wing model at angles of attack ranging from 13 to 30 degrees, Mach numbers between 0.4 and 0.8, total temperatures between 83 and 101 K and total pressures between 1.3 and 5.0 atmospheres. Fog was generated in the test section by operating near the freestream saturation temperature and was illuminated by an intense sheet of light from a 15-mW helium-neon laser. The visualized flow field was recorded by video and still cameras.

The vapor-screen photographs presented herein depict the vortex region as a diffuse light area against a dark background, while it is usually observed as a well-defined dark "hole" against a light background (e.g., water-vapor screens in supersonic flow). It appears possible that vortex bursting has occurred upstream of the light sheet, resulting in a vapor-screen photograph showing a diffuse vortex core. It is also possible that the observed vapor screen is peculiar to subsonic flow, as shown in References 12 and 16. The feasibility of using nitrogen fog in conjunction with the vapor-screen technique has been demonstrated; however, additional research is required before such a technique is rendered operational.

It is recommended that additional tests be executed subject to the following considerations:

1. Orientation of the light sheet in a more photographically suitable manner - preferably, normal to the line of sight of the photographic equipment.

2. Application of fiber optics technology to the generation and/or recording of the vapor screens in order to facilitate the flow-visualization process.
3. Provision for traversing the light screen in the freestream direction in order to determine the location where vortex bursting occurs.
4. Provision for varying the intensity of the laser source.
5. Testing of half-span delta-wing models with higher sweep angles in order to provide a wider range of angles of attack over which the vortex-burst location is downstream of the trailing edge and
6. Testing of additional model geometries corresponding to other types of vortex flows.

REFERENCES

1. Hunter, W. W., Jr.; and Foughner, J. T., Jr. (Editors): Flow Visualization and Laser Velocimetry for Wind Tunnels. NASA CP-2243, 1982.
2. Bengelink, R. L.: Surface Flow Visualization Requirements for Testing in the NTF. Flow Visualization and Laser Velocimetry for Wind Tunnels, NASA CP-2243, 1982.
3. Kell, D. M.: A Surface Flow Visualization Technique for Use in Cryogenic Wind Tunnels. Aeronautical Journal, November 1978, pp. 484-487.
4. Crowder, J. P.: Surface Flow Visualization Using Indicators. Flow Visualization and Laser Velocimetry for Wind Tunnels, NASA CP-2243, 1982.
5. Crowder, J. P.: Add Fluorescent Minitufts to the Aerodynamicist's Bag of Tricks. Astronautics and Aeronautics, November 1980, pp. 54-56.
6. Crowder, J. P.: In-Flight Propeller Flow Visualization Using Fluorescent Minitufts. Flow Visualization and Laser Velocimetry for Wind Tunnels, NASA CP-2243, 1982.
7. Burner, A. W.; Snow, W. L.; Goad, W. K.; Helms, V. T.; and Gooderum, P. B.: Flow Field Studies Using Holographic Interferometry at Langley. Flow Visualization and Laser Velocimetry for Wind Tunnels, NASA CP-2243, 1982.
8. Rhodes, D. B.; and Jones, S. B.: Flow Visualization in the Langley 0.3-Meter Transonic Cryogenic Tunnel and Preliminary Plans for the National Transonic Facility. Flow Visualization and Laser Velocimetry for Wind Tunnels, NASA CP-2243, 1982.
9. Plentovich, E. B.: Status of Orifice-Induced Pressure Error Studies. AIAA Paper No. 84-0245, AIAA 22nd Aerospace Sciences Meeting, January 1984.

10. Bisplinghoff, R. L.; Coffin, J. B.; and Haldeman, C. W.: Water Fog Generation System for Subsonic Flow Visualization. AIAA Journal, Vol. 14, No. 8, August 1976, pp. 1133-1135.

11. Haldeman, C. W.: Suggested Modification of Fog Flow Visualization for Use in Cryogenic Wind Tunnels. Proceedings First International Symposium on Cryogenic Wind Tunnels (Southampton, England, April 3-5, 1979), University of Southampton, 1979, pp. 21.1-21.3.

12. McGregor, I.: The Vapor Screen Method of Flow Visualization. Journal of Fluid Mechanics, Vol. 11, Pt. 4, December 1961, pp. 481-511.

13. Ray, Edward J.; Ladson, Charles L.; Adcock, Jerry B.; Lawing, Pierce L.; and Hall, Robert M.: Review of Design and Operational Characteristics of the 0.3-Meter Transonic Cryogenic Tunnel, NASA TM-80123, September 1979.

14. Boyden, R. P.; and Johnson, W. G., Jr.: Results of Buffet Tests in a Cryogenic Wind Tunnel, NASA TM-84520, 1982.

15. Wentz, W. H., Jr.; and Kohlman, D. L.: Wind Tunnel Investigations of Vortex Breakdown on Slender Sharp-Edge Wings. NASA CR-98737, 1968.

16. Jorgensen, L. H..: Prediction of Static Aerodynamic Characteristics for Slender Bodies Alone and With Lifting Surfaces to Very High Angles of Attack. NASA TR R-474, September 1977.

Table 1. Run Schedule for Vapor Screen Flow Visualization Experiments in the 0.3-m TCT

Date	Run no.	Point no.	M	α (deg.)	p_t (atm.)	T_t (K)
7/18/84	1	1	0.8	13	1.2	94.0
		2				92.0
		3				90.0
		4				89.0
		5				88.0
		6				87.0
		7				86.0
		8				85.0
		9				84.0
		10				85.5
7/18/84	2	11	0.8	10	1.2	85.5
		12		12		
		13		14		
		14		16		
		15		17		
		16		17		
		17		18		
		18		19		
		19		20		
		20		21		
		21		22		
		22		24		
		23		24		
		24		26		
		25		30		
7/18/84	3	26	0.6	10	1.2	83.0
		27		12		
		28		14		
		29		16		
		30		17		
		31		17		
		32		18		
		33		19		
		34		20		
		35		21		

Table 1. Continued.

Date	Run no.	Point no.	M	α (deg.)	p_t (atm.)	T_t (K)
7/18/84	3	36	0.6	21	1.2	83.0
↓	↓	37	↓	22	↓	↓
		38		24		
		39		26		
		40		30		
7/19/84	4	41	0.6	30	1.3	85.3
↓	↓	42	↓	25	↓	85.3
		43		20		84.5
		44		15		83.2
		45		15		100.0
7/19/84	5	46	0.8	30	1.7	93.0
↓	↓	47	↓	30	↓	88.0
		48		25		88.5
		49		20		89.5
7/20/84	6	50	0.8	20	3.0	95.0
↓	↓	51	0.6	20	↓	92.3
		52	0.5	20		90.7
		53	0.6	15		92.0
		54	0.6	20		92.0
		55	0.6	25		92.0
7/20/84	7	56	0.6	18	5.0	98.0
↓	↓	57	0.8	13	↓	100.8
		58	0.4	25		95.6

Table 2. Tunnel Conditions for Flow Visualization Photographs

Point no.	M	α (deg.)	p_t (atm.)	T_t (K)	Fig. no.
44	0.6	15	1.3	83.2	9
43	↓	20	↓	84.5	↓
42	↓	25	↓	85.3	↓
41	↓	30	↓	85.3	↓
53	0.6	15	3.0	92.0	10
54	↓	20	↓	↓	↓
55	↓	25	↓	↓	↓
52	0.5	20	3.0	90.7	11
51	0.6	↓	↓	92.3	↓
50	0.8	↓	↓	95.0	↓

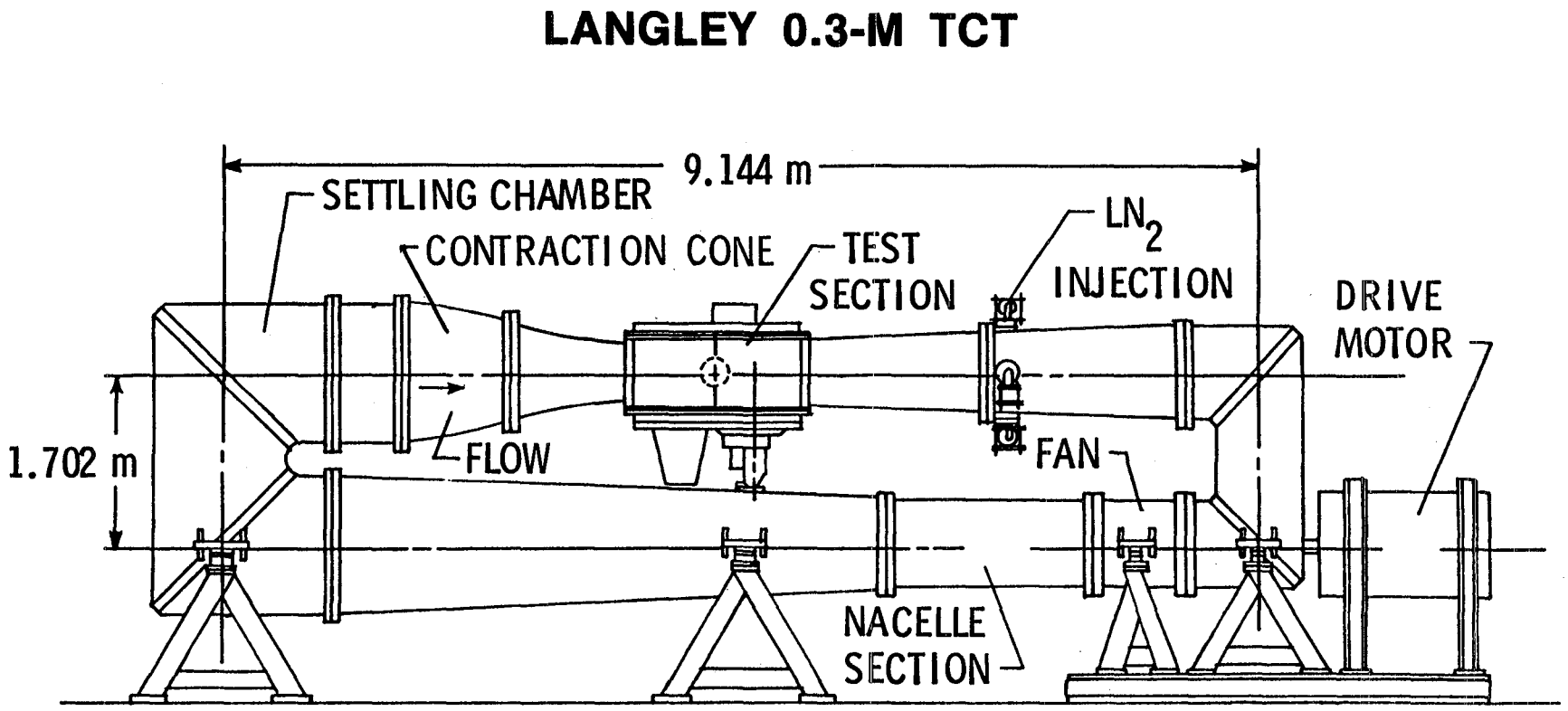

Figure 1. Schematic of the NASA 0.3-Meter Transonic Cryogenic Tunnel

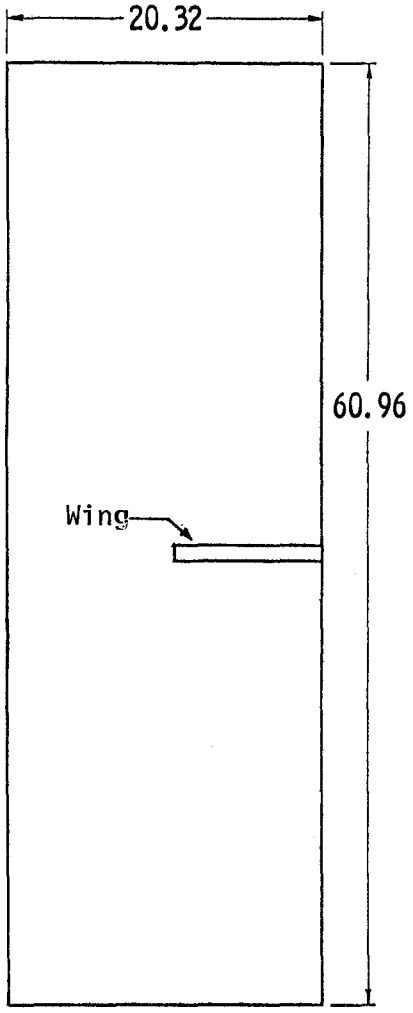

(a) Two-Dimensional Test Section

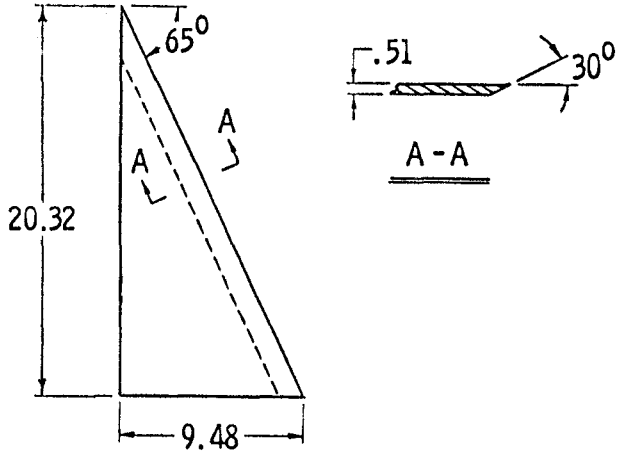

(b) Delta Wing

Figure 2. Sketches Showing End View of Test Section of the 0.3-Meter Transonic Cryogenic Tunnel and the Delta-Wing Model (linear dimensions in cm) (Reference 14)

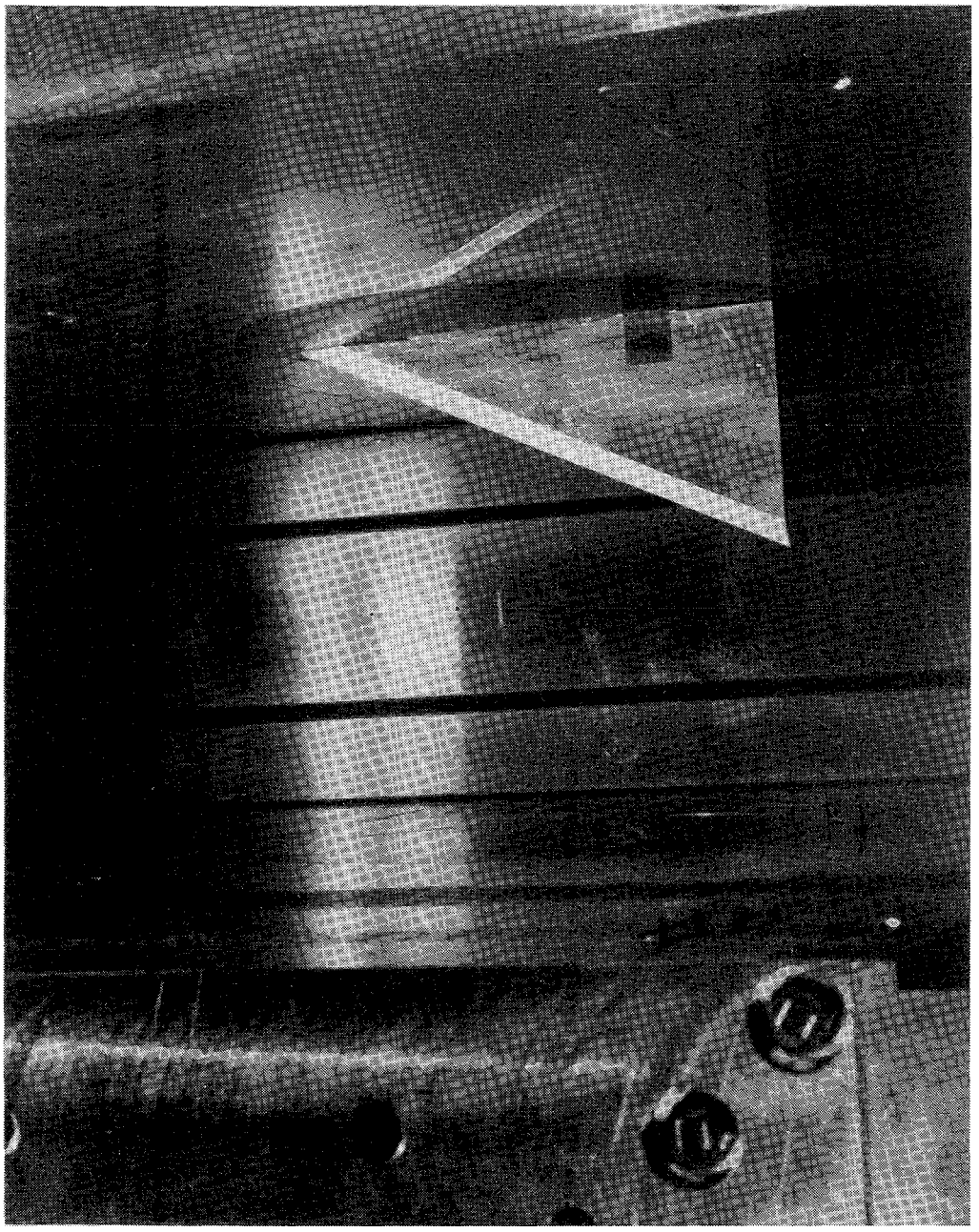

Figure 3. Delta-Wing Model Mounted in the 0.3-Meter Transonic Cryogenic Tunnel with Slotted Floor in Background (Reference 14)

Figure 4. P_{t_m} vs. α for the 65-deg. Delta-Wing Model with Various Safety Factors

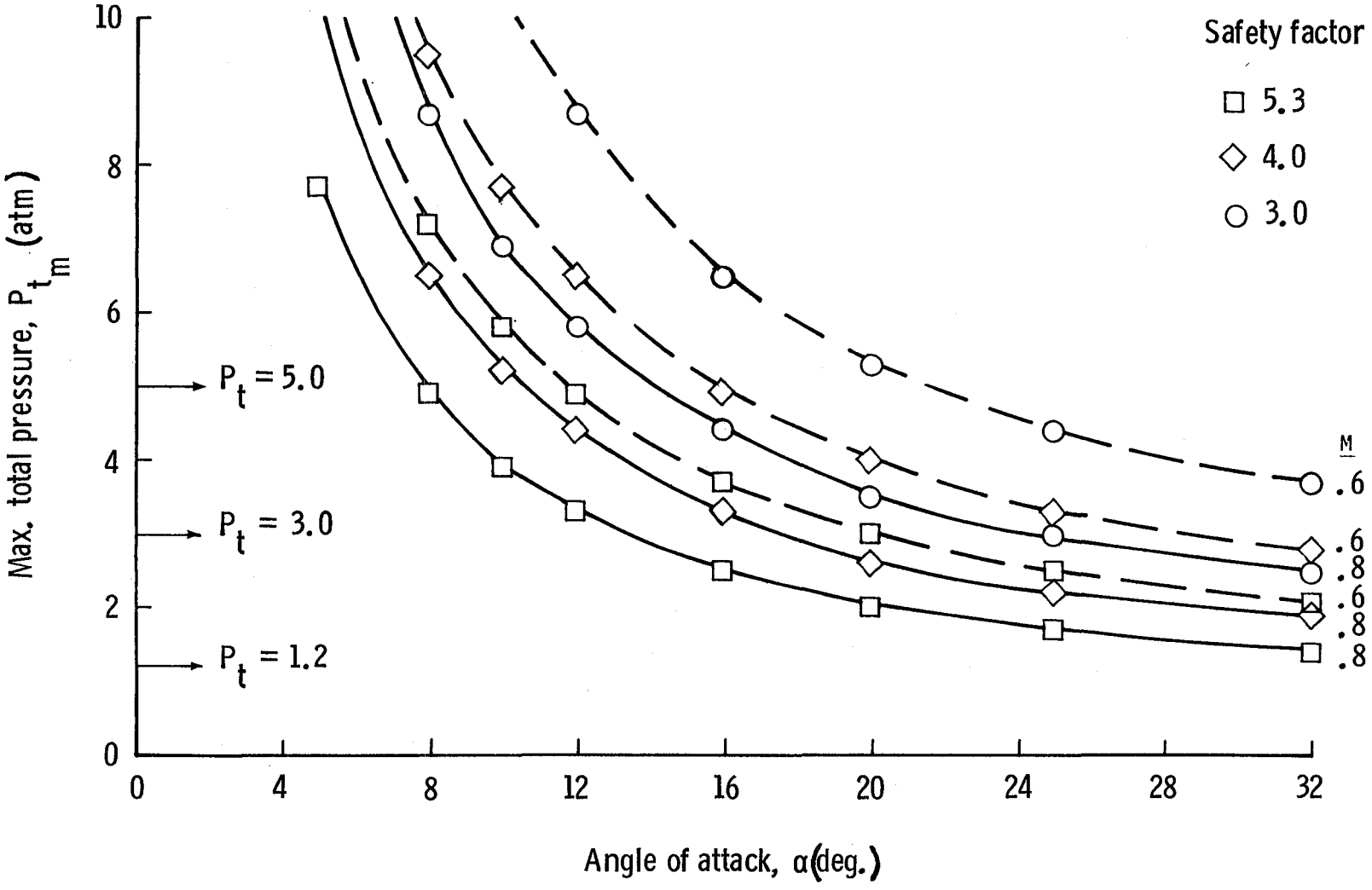

Figure 5. Vortex Burst Location vs. Angle of Attack at Various Delta Wing Sweep Angles (Ref. 15)

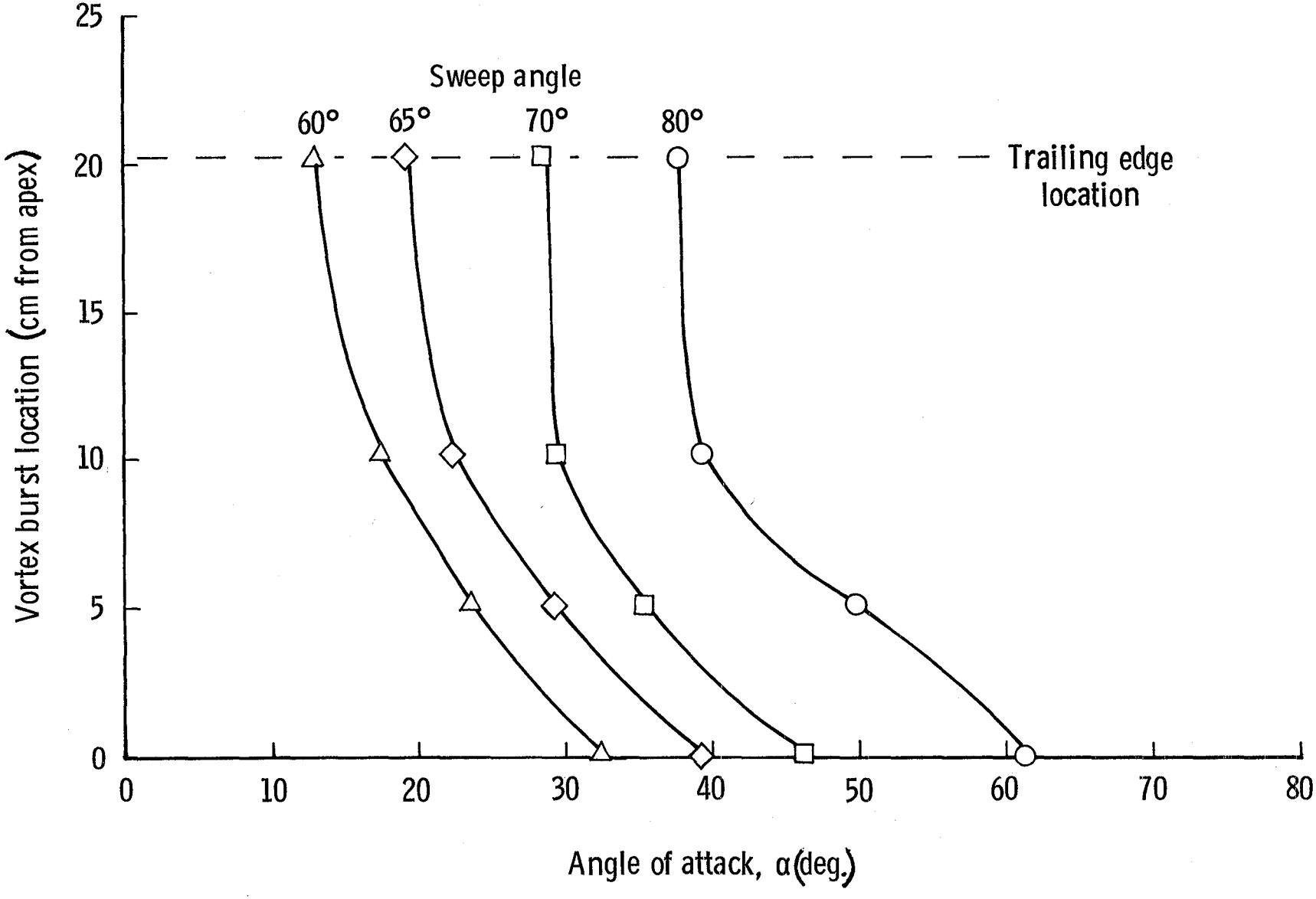

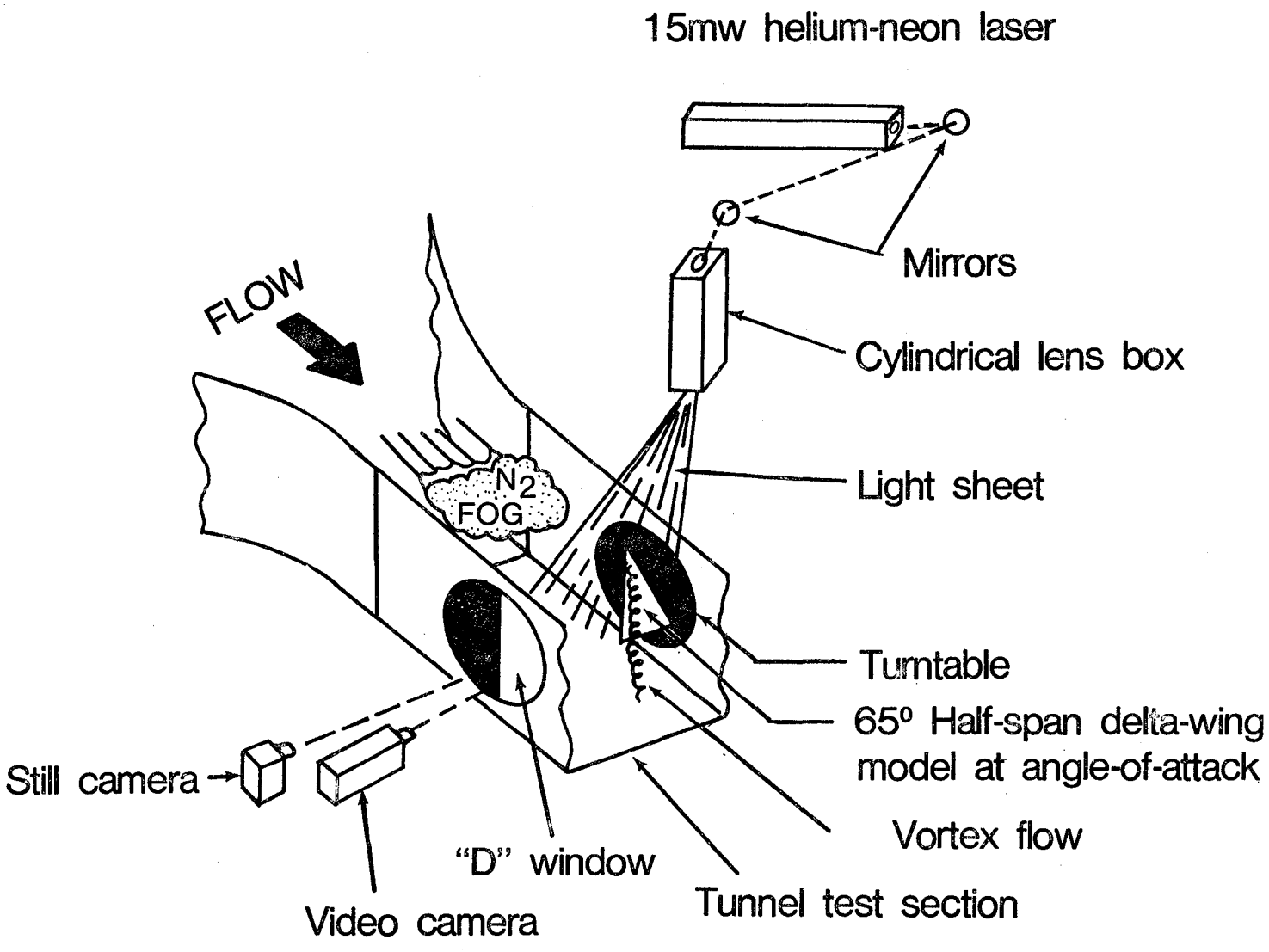

Figure 6. Schematic of Illumination System Used in Vapor Screen Experiments

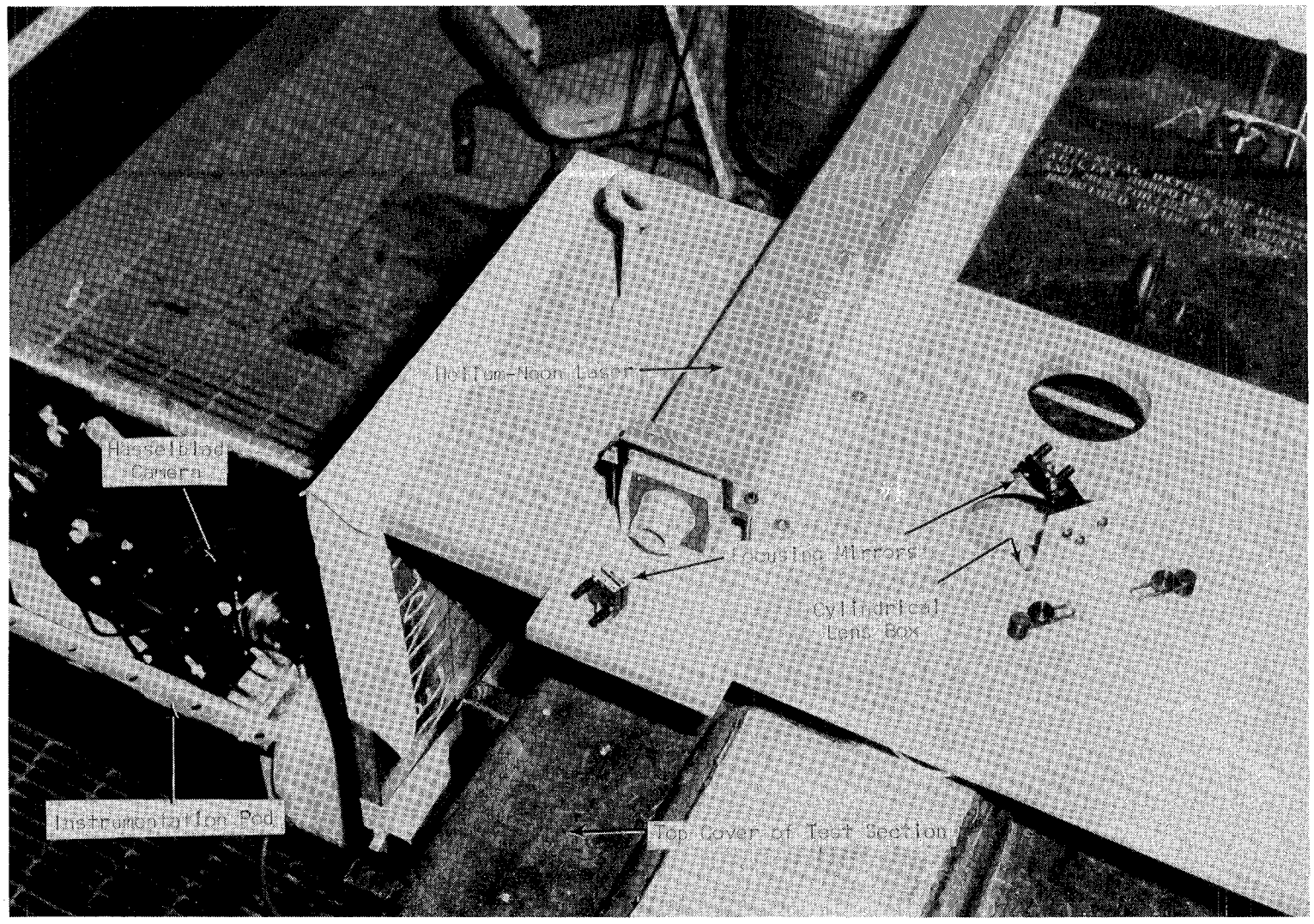

Figure 7. View of Illumination and Photographic Systems Showing Orientation of Components

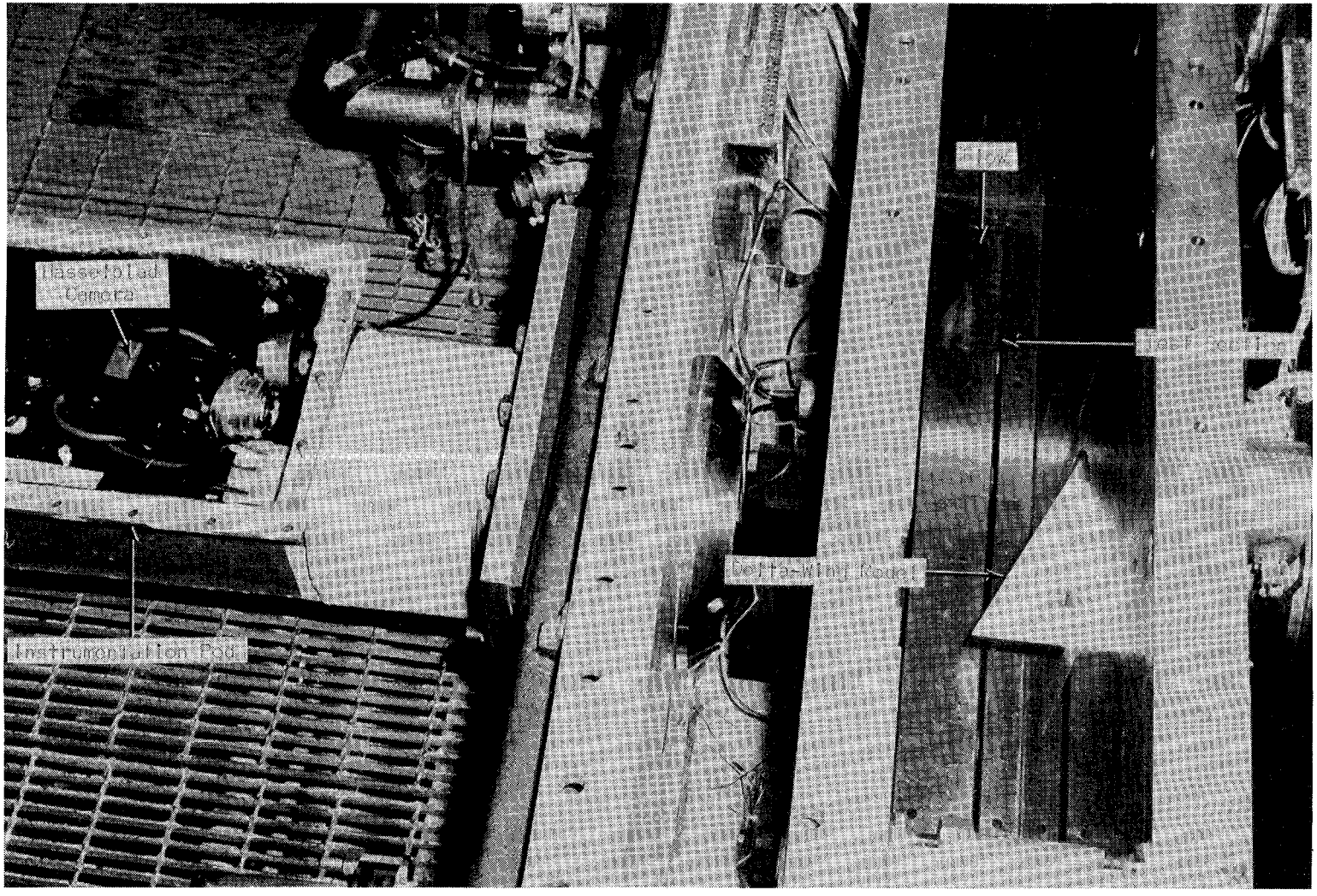

Figure 8. Top View of Test Section Showing Orientation of the Still Camera with respect to the Delta-Wing Model

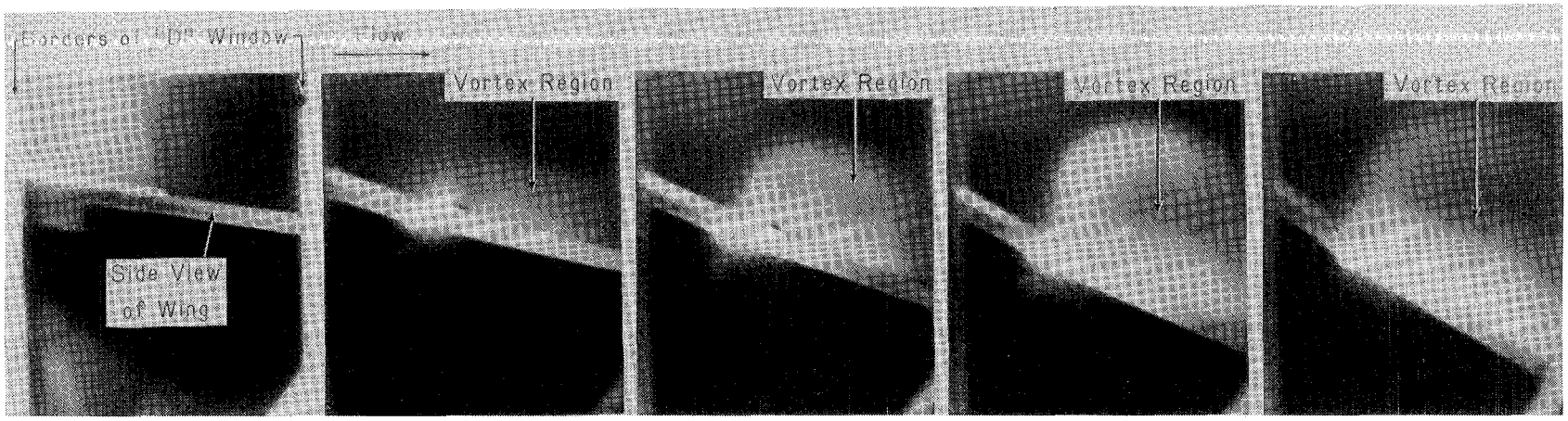

A. No Flow

B. $\alpha = 15°$, $T_t = 83.2K$

C. $\alpha = 20°$, $T_t = 84.5K$

D. $\alpha = 25°$, $T_t = 85.3K$

E. $\alpha = 30°$, $T_t = 85.3K$

Figure 9. View Through "D" Window of the Flow over a 65-Deg. Half-Span Delta-Wing Model at Various Angles of Attack ($M = 0.6$, $P_t = 1.3$ atm.)

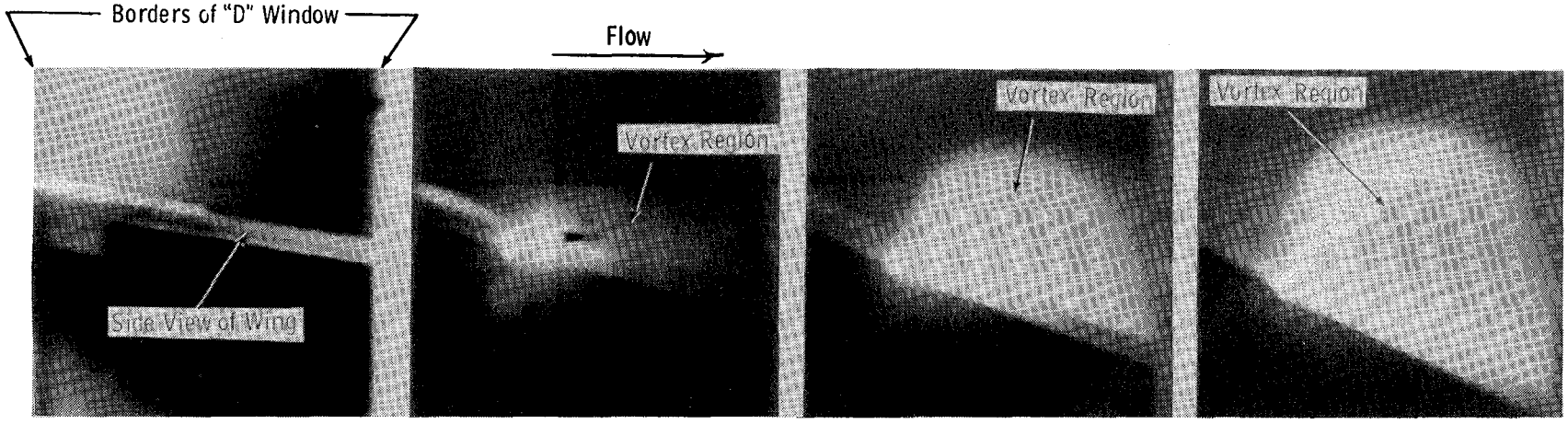

FIGURE 10. VIEW THROUGH "D" WINDOW OF THE FLOW OVER A 65-DEG. HALF-SPAN DELTA WING AT VARIOUS ANGLES OF ATTACK (M=0.6, p_T=3.0 ATM. AND T_T=92.0 K)

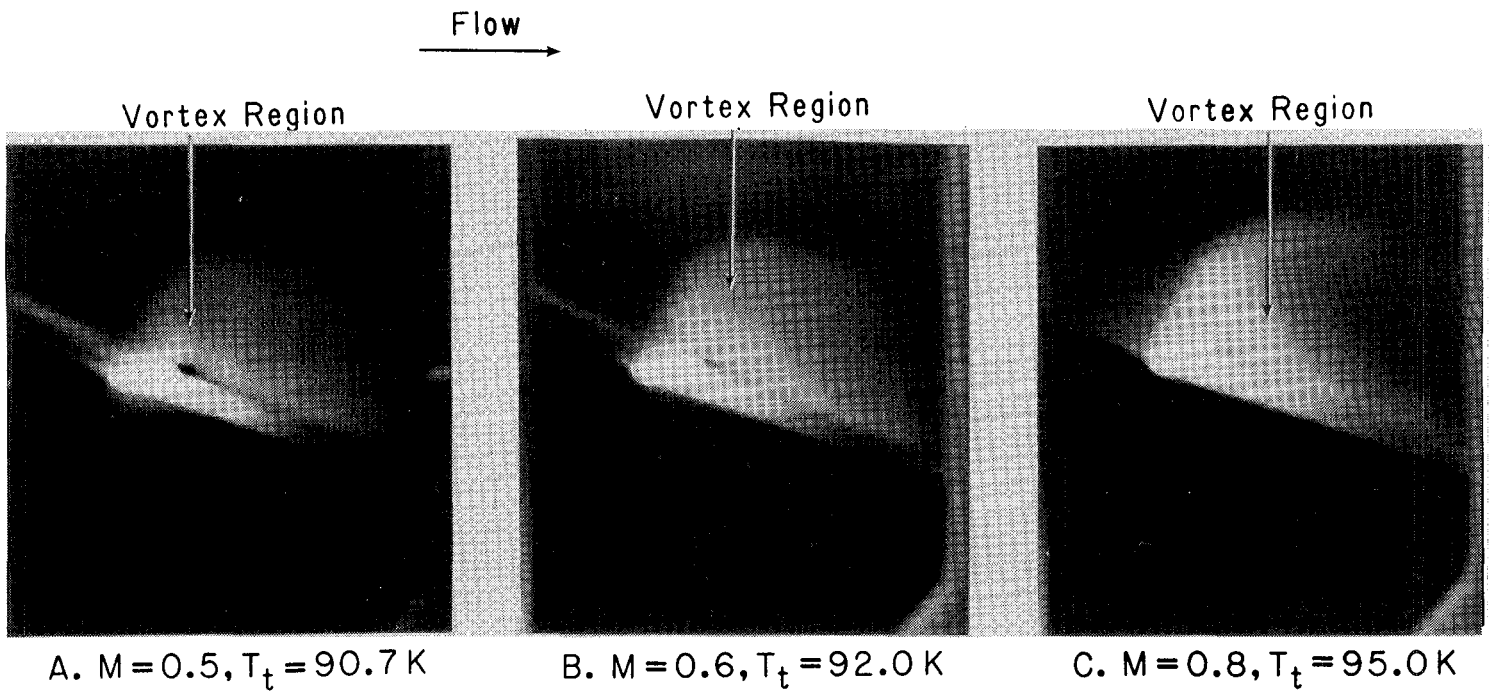

Figure 11. View through "D" Window of the Flow over a 65-deg. Half-Span Delta-Wing Model at $\alpha = 20°$ and $P_t = 3.0$ atm.

Figure 12. Conditions for Photographically Suitable Vapor Screens (M=0.6, P_t=1.3 atm.)

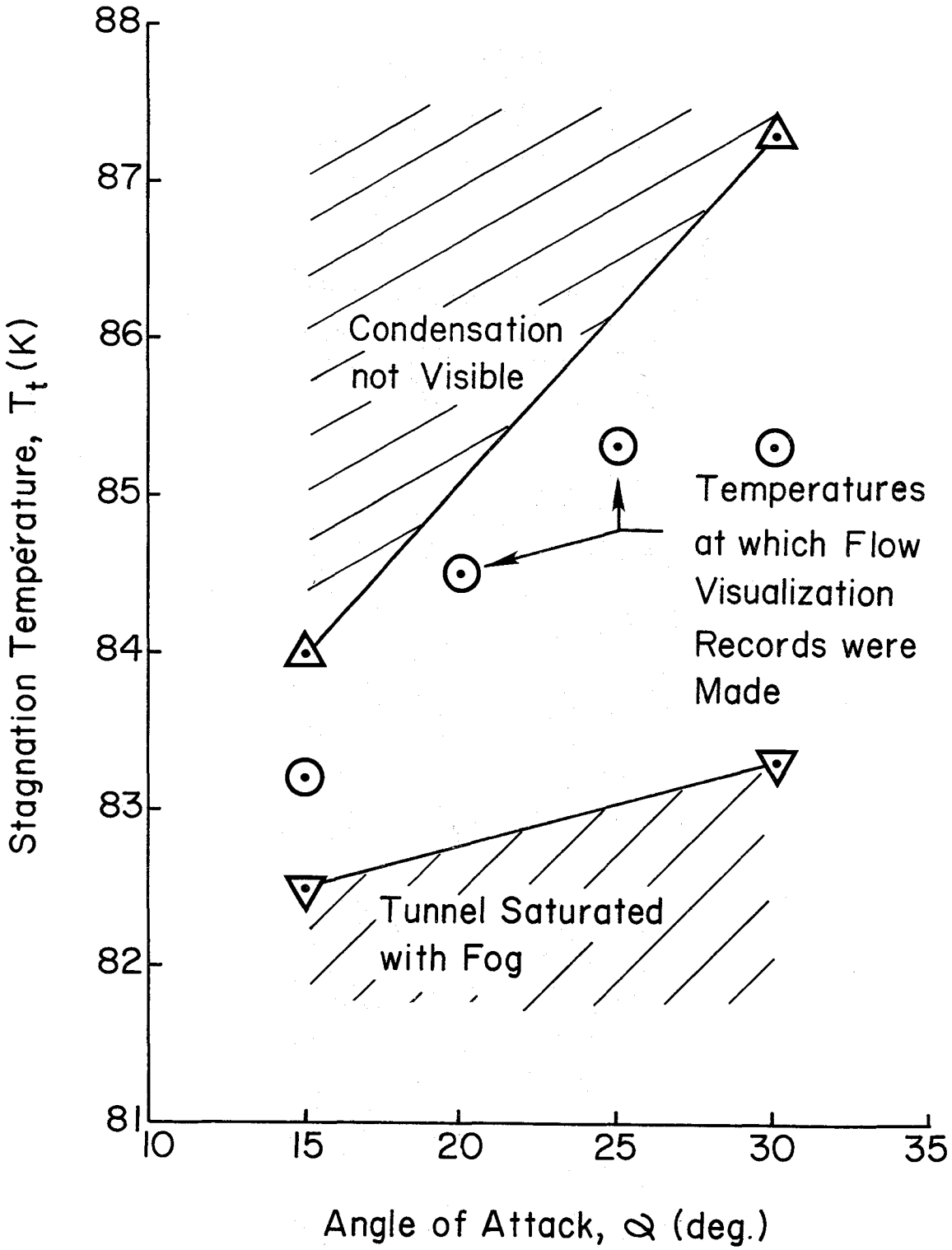

1. Report No.	2. Government Accession No.	3. Recipient's Catalog No.
NASA CR-3984		

4. Title and Subtitle	5. Report Date
Vapor-Screen Flow-Visualization Experiments in the NASA Langley 0.3-m Transonic Cryogenic Tunnel	May 1986
	6. Performing Organization Code
7. Author(s)	8. Performing Organization Report No.
Gregory Vincent Selby	
	10. Work Unit No.
9. Performing Organization Name and Address	11. Contract or Grant No.
Old Dominion University Norfolk, Virginia 23508	NGT 47-003-029
	13. Type of Report and Period Covered
12. Sponsoring Agency Name and Address	Contractor Report
National Aeronautics and Space Administration Washington, DC 20546-0001	14. Sponsoring Agency Code 505-60-21

15. Supplementary Notes

Langley Research Center Technical Monitor: Robert M. Hall

16. Abstract

The vortical flow on the leeward side of a delta-wing model has been visualized at several different tunnel conditions in the NASA Langley 0.3-Meter Transonic Cryogenic Tunnel using a vapor-screen flow-visualization technique. Vapor-screen photographs of the subject flow field are presented and interpreted relative to phenomenological implications. Results indicate that the use of nitrogen fog in conjunction with the vapor-screen technique is feasible.

17. Key Words (Suggested by Author(s))	18. Distribution Statement
Flow visualization Condensation Cryogenic wind tunnel	Unclassified - Unlimited Subject Category 02

19. Security Classif. (of this report)	20. Security Classif. (of this page)	21. No. of Pages	22. Price
Unclassified	Unclassified	38	A03

For sale by the National Technical Information Service, Springfield, Virginia 22161

NASA-Langley, 1986

End of Document